



University
of Glasgow

Avanaki, M.R.N., Podoleanu, A.G., Price, M.C., Corr, S.A., Mazrae Khoshki, R., and Hojjatoleslami, S.A. (2012) Phantoms for performance assessment of optical coherence tomography systems. Proceedings of the SPIE - The International Society for Optical Engineering, 8229 . 82290W-1-82290W-9. ISSN 0277-786X

Copyright © 2012 SPIE

A copy can be downloaded for personal non-commercial research or study, without prior permission or charge

The content must not be changed in any way or reproduced in any format or medium without the formal permission of the copyright holder(s)

When referring to this work, full bibliographic details must be given

<http://eprints.gla.ac.uk/76379/>

Deposited on: 7 March 2013

Enlighten – Research publications by members of the University of Glasgow
<http://eprints.gla.ac.uk>

Phantoms for performance assessment of optical coherence tomography systems

Mohammad R. N. Avanaki^{*a,b}, Adrian Gh. Podoleanu^b, Mark C. Price^c, Serena A. Corr^d, Rohollah Mazrae Khoshki^e and S. A. Hojjatoleslami^a

^aNeurosciences and Medical Image Computing Group, University of Kent, United Kingdom, CT2 7PD

^bApplied Optics Group, School of Physical Sciences, University of Kent, United Kingdom, CT2 7NH

^cCentre for Astrophysics and Planetary Science, University of Kent, United Kingdom, CT2 7NH.

^dFunctional Materials Group, School of Physical Sciences, University of Kent, United Kingdom, CT2 7NH.

^eElectronics Department of Razi University, Kermanshah, Iran.

ABSTRACT

In this paper, we describe the procedures to make epoxy resin and agarose phantoms designed using Mie scattering calculations. The phantoms are constructed to be used in the estimation of point spread function (PSF) of an optical coherence tomography (OCT) and evaluation of optical properties extraction (OPE) algorithm.

Keywords: optical coherence tomography, optical phantom, virtual tissue, optical properties extraction algorithm, point spread function (PSF).

1. INTRODUCTION

A phantom is a virtual tissue with well controlled optical properties (e.g. refractive index, scattering coefficient, anisotropy factor and absorption coefficient), which can be constructed in a solid or liquid state depending on the application [1]. Phantoms are widely used for testing the design, optimization, and performance evaluation of optical systems. In optical imaging systems in particular, phantoms are used for the measurement and evaluation of system parameters such as longitudinal and transverse resolutions, image contrast, point spread function (PSF), system sensitivity, system differentiability (between two types of tissue), and system detection of a tissue containing a certain concentration of a particular component. The field of phantom construction has evolved considerably over the past several decades, and standard and consistent, manufacturing procedure need to be established for many material combinations to avoid wasting time and resources on inaccurate design. The increase of interdisciplinary collaboration between physicists, chemists and computer scientists, can help establishing better procedures. Some of the phantom construction recipes for optical imaging applications can be found in [2-10] and a comprehensive review has been published by Pogue *et al.* [11]. Huang *et al.*, have reported the use of metal microspheres, particularly gold particles, to make the phantoms [12]. Phantom construction literature is comprehensive, but there remain many practical issues for specific applications.

2. MATERIAL AND METHODS

2.1. Optical properties

In a solid matrix containing particles within a transparent hardener, the scattering coefficient, μ_s [mm^{-1}], is defined as the product of the volume density of the particles, ρ_s [mm^{-3}], with the scattering cross-section, σ_s [mm^2], which is the incident beam diameter at the probing depth [13-14].

$$\mu_s = \rho_s \sigma_s \quad (1)$$

In a medium where the volume fraction of scatterers is 20% or less, equation (1) is valid. However, when the fraction becomes higher than 50%, equation (2) is used [14].

$$\mu_s = \frac{\phi(1-\phi)\sigma_s}{V} \quad (2)$$

Where, ϕ [mm^3] is the volume of the scatterers and V [mm^3] is the volume of a single scatterer. Similarly, the absorption coefficient, μ_a , is obtained using the product of the volume density of the chromophores in the phantom, ρ_a , and absorption cross-section, σ_a [14]. The absorption coefficient is then used in the Beer-Lambert law to model the attenuation of incident light. The Beer-Lambert law shows that the variation of optical power attenuates exponentially with the travelled path length [14]. The relation between the reflected back light intensity, I , and the incident light intensity, I_0 , is given by equation (3).

$$I = I_0 e^{-\mu_a L} \quad (3)$$

where L is the optical path length and μ_a is the absorption coefficient of the specimen [14]. The anisotropy factor [15], g , is another optical property related to the angular probability of the scattered light to that of the incident light, represented as the cosine of the averaged scattering angle. There are other optical properties that can also characterise the tissue [16]: (1) the reduced scattering coefficient, $\mu_s' = \mu_s(1-g)$. The purpose of using μ_s' for characterising a tissue is to describe the diffusion of photons in a random walk with a step size of $1/\mu_s'$ [cm] where each step has an isotropic scattering [13]. Such a description is equivalent to the description of photon movement using many small steps of $1/\mu_s$ where each involves only a partial deflection angle, θ if there are many scattering events before an absorption event, i.e., $\mu_a \ll \mu_s'$. This situation of scattering-dominated light transport is called the diffusion regime; (2) the total attenuation coefficient, μ_t , given by $\mu_t = \mu_s + \mu_a$; (3) the mean free path, presented by $1/\mu_t$; (4) the optical path, $\tau = \mu_t \times z$ which identifies whether the regime is single scattering, $\tau < 1$, multiple scattering, $1 < \tau < 10$, or a diffusion regime, $\tau > 10$, Z , is the lateral distance travelled by the beam, and (5) the complex index of refraction, \tilde{n} , defined as $\tilde{n} = n + i\kappa$, where n is the refractive index of the material and is related to the phase velocity and, κ , the extinction coefficient relating the absorption due to dielectric loss and permittivity characteristics of the material [16].

2.2. Phantom design

Phantom design requires the use of Mie scattering theory to describe the interaction of photons with the particles embedded within phantom's matrix. Mie theory is an analytical solution of Maxwell's equations for modelling the scattering of spherical particles in a homogeneous material [17]. A MATLAB version of Mie theory for homogeneous spheres was prepared by C. Maetzler in 2002, based on the appendix in Bohren and Huffman, 1982 [14]. Another Mie calculator is provided by OMLC group and used by many researchers [18-20]. Mie theory cannot be applied to closely packed particles where near field interactions occur. To utilise Mie theory correctly, the formula $r \gg d^2 / 2\pi\lambda$ has to be satisfied where d [μm] is the diameter of the particles, r [μm] is the distance between observer and the particles, and λ [μm] is the central wavelength of the incident radiation [17]. When the diameter of the particles in the phantom becomes very small ($d < 0.1\lambda$), Rayleigh scattering contributes significantly to the total scattering [17]. However, for particle sizes larger than the wavelength, ($d > \lambda$) Mie scattering dominates. Mie scattering is not strongly wavelength dependent, whereas Rayleigh scattering is inversely proportional to the wavelength of the light [17]. Mie calculations require knowledge of the refractive index of the embedded scatterers and the principle matrix material of the phantom at the specific wavelength of interest, λ . The refractive index, n , of a material can be estimated using the Sellmeier equation and the refractive index of the material at two other wavelengths. The refractive index of the material at two other wavelengths can be found in the literature. The Sellmeier equation is defined as follows:

$$n = 1 + a\lambda^2 / (\lambda^2 - \lambda_0) \quad (4)$$

where a and λ_0 are Sellmeier coefficients [21]. The complex refractive index of the embedded scattering microspheres can be measured using the approach described in [22]. In our study however, we chose materials with well known values for the complex refractive index, found in the literature.

A phantom with the desired optical properties can thereby be designed using Mie theory [18, 22-23]. The input parameters for the Mie calculation are the microsphere (scatterer) diameter (m), the working wavelength in vacuum (m), the complex refractive index of the microspheres, refractive index of the principle matrix material, and the concentration of the scattering microspheres (μm^{-3}). The concentration is computed as follows: if we use M ml of the microsphere suspended in K grams of the principle matrix material [24], the volume fraction of the spheres is $f_v = M/K$. The concentration of the scatterers is then calculated via $\rho_s = f_v / ((4/3)\pi a^3)$ (a is the diameter of the spheres [μm]). Scattering and polarization patterns are the main outputs of the Mie calculation. Here we only use the scattering information which includes the scattering coefficient and scattering angle in our analyses. The solid phantom is then constructed by mixing the correct proportions of the scattering material (as obtained from Mie calculations) in an appropriate hardener. Beside the approach described to design the phantom, one may design the phantom based on what materials are available [11].

To validate the optical properties of the prepared phantom, an integrating sphere [25] is used. The integrating sphere is an optical component consisting of a hollow cavity with its interior coated for high diffuse reflectivity having relatively small holes as needed for entrance and exit ports. It is used with light source and a detector for optical power measurement. Integrating sphere is used in combination with a mathematical approach, e.g. adding-doubling algorithm [25]. In the adding-doubling algorithm, the light distribution in the turbid media is evaluated by analyzing the total reflection from, and transmission through a sample. In addition to the integrating sphere, the

optical properties extraction (OPE) algorithm which is based on the Extended Huygens-Fresnel (EHF) theorem can be used to measure the optical properties of the phantoms [26-27]. With OPE software, the image recorded by an imaging modality, OCT, is used along with an image processing algorithm to obtain the optical properties. Other studies have also been undertaken for validating and verifying the optical properties of the phantoms such as spatially resolved diffuse reflectance method or time-resolved methods [28].

2.3. Imaging system configuration

The OCT system employed for imaging the phantom samples in this study is an *en-Face* time domain OCT which uses a dynamic focus scheme. The details of the design and implementation are similar to the design described in [36]. With dynamic focus, the coherence gate is synchronised with the confocal gate; hence, the transverse resolution is conserved throughout the depth range and an enhanced signal is returned from all depths. We have taken advantage of the simplification introduced by the DF-OCT system, where there is no need to deconvolve the reflectivity profile with the confocal gate profile, as this last one is constant throughout the depth. DF-OCT system is especially designed for use in applications where a high lateral resolution in a large scan depth is required.

3. PHANTOM CONSTRUCTION

3.1. Material selection

In the construction of a phantom three main components are required: (1) the scatterer, (2) the absorber, (3) the principle matrix material. The relative amount of each of these materials is determined using Mie calculation.

Scatterers:

In previous studies, different materials have been employed in the construction of phantoms as scatterers, namely; latex, silica, TiO₂, Al₂O₃, PMMA, melamine, polyester and polystyrene [11]. In many cases, polystyrene microspheres are chosen due to their ready availability, low cost, reproducibility, lifetime and chemical compatibility with the phantom matrix material. Spherical metallic particles can also be employed as scatterers. These particles are stable over time, compatible with many principle matrix materials, and very flexible in terms of available size, shape, and composition. Amongst the generally available metallic microspheres (silver, gold, nickel and iron) colloidal gold microspheres with 30% glass as seed and 70% coated gold material are suitable for some phantom study as they can easily be dispersed in an epoxy-resin matrix and also they are highly reflective [12]. With gold particles one can tune both the scattering and absorption coefficients of a phantom [12]. In addition to the gold microspheres, gold microrods give scattering and absorption coefficients similar to that of skin, although using the general Mie formulation is not feasible in this case as the general Mie calculation works for spherical particles [29]. We have experimented with phantoms in which we used one of the following scatterers: titanium dioxide (T8141, provided by Sigma-Aldrich), Polystyrene (white and black dyed), silica microspheres (provided by Polysciences), super white polyester pigment microspheres (provided by Duke scientific), and gold microspheres (provided by Pfizer).

Absorber:

Absorber is used to add absorption property into the phantom, different materials can be used [11]: blood, which provides realistic tissue spectra and oxygenation function, but survives less than a day, also it has associated Health and Safety issues in handling, ink (India ink), that has flat absorption spectra, but remains stable for only a few days, molecular dyes, which provide a spectra with peak absorption at a particular wavelength and survive for months, and fluorophore, which is compatible with aqueous dissolving compounds and are stable for a few weeks. One of the

general problems with the absorbers [1-2] is that they are mainly designed for visible light and hence they are invisible in the infrared range. This means that the absorption coefficient of these absorbers in the wavelength range 740nm and upwards, is low [17]. In our experiments India ink and a molecular dye are used as absorbers. The India ink is the ink that is widely used for printing. We used Sennelier Indian ink (Supplier: Sennelier, France [30]). Another absorber that we used mostly in our phantom studies is Pro jet 900NP (Supplier: AVECIA (Manchester, UK), formally known as Zeneca Ltd). Pro jet 900NP is a phthalocyanine infrared absorber, having a broad absorption profile with a maximum absorption at approximately 900nm. The product is supplied as a solid powder and has good solubility in non-polar solvents with excellent chemical and thermal stability. The absorber was used to construct the phantoms for the wavelength 1300 nm. The lower absorption coefficient of the absorber at 1300 nm was compensated for by adding higher amount of the absorber to the phantom matrix. A comparison between the absorption spectrum of India Ink and Pro jet 900NP are given in Figure 1.

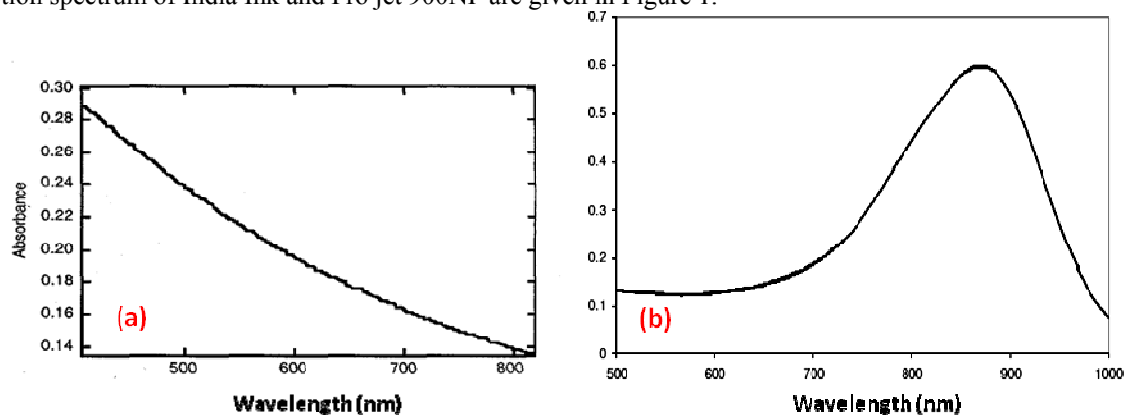


Figure 1. Absorption spectrum of absorbers. (a) India ink [31], (b) Pro jet 900NP [32]

Principle matrix material:

Epoxy-resin and agarose are two materials used in our experiments for hardening. Epoxy-resin is a low viscosity un-polymerized liquid resin, which forms polyester on addition of a catalyst and cures at room temperature. Agarose is a polysaccharide obtained from agar which forms an inert matrix. In this study, we used Araldite resin (MY753 provided by [Aeropia Chemical Supplies](#)), resin (Araldite DBF) and AraDVR hardener (XD716) both provided by [Robnor resins](#) [24]. The agarose (MB1200) was provided by [MELFORD](#) [33].

3.2. Phantom recipes

According to the hardener material, two types of phantoms are defined:

Epoxy-resin phantoms

To make the epoxy-resin phantoms, three parts resin and a pre-determined amount of scatterers- depending on the required concentration of the scatterers- are agitated by an electrical mixer for 15 minutes. The scatterers are microspheres that are purchased in powder or aqueous. The aqueous particles are freeze-dried. The super white microspheres do not need freeze drying as they are soluble in epoxy-resin. The mixture is then placed in an ultrasonic bath for 20 minutes. The ultrasound bath disperses the particles within the resin to ensure a homogenous matrix. One part hardener is then added. The sample is once again agitated by the electrical mixer for a further 15

minutes and then immersed in the ultrasonic bath for a further 20 minutes. The resultant solution is poured into a capped Petri dish. The dish is placed in an oven for 12 hours at 60 °C to set. The mentioned mix ratios between the XD716 and DBF is of great importance as if it is not provided, the phantom will be 'dough-like' and cannot be setup and used in the OCT setup with vertical sample arm [34].

Agarose phantoms

Polystyrene microspheres are usually supplied as water-based suspensions. The microspheres with water are not soluble in epoxy-resin. Moreover, freeze-drying of the particles may alter their optical properties and make them aggregate together within the epoxy resin matrix producing an inhomogeneous mix. In order to address these potential problems we use an agarose matrix. With agarose, the setting time is reduced from 12 hours to 30 minutes and the aqueous microspheres are easily miscible in the matrix. To make this type of phantom, MilliQ water (with a conductivity of 18.2 Mohm-cm) is boiled. Agarose (1 mg) is added to the water (1 mL) and is stirred over a low heat, until it homogenised. The temperature should be controlled around 80°C to prevent the solution become cloudy or burnt. The concentration of agarose determines the time required for the solution to set. Too much agarose causes strip-like elements to appear in the phantom; too little and the setting time is increased. Owing to this, we use agarose with the concentration of 1mg in 1mL water. The microsphere suspension is added when there are no visible strip-like elements in the agarose solution. This process takes approximately 5 minutes. Particle dispersion is ensured by ultrasonication for 10 minutes at 60°C. The final sample is poured into a Petri dish to set. The matrix may take 10 - 30 minutes to set depending on the amount of agarose added. Agarose phantoms are constructed quickly and easily, but may not be useful in every application as the state of the phantom is jelly-like. Moreover, the concentration of the scatterers changes with time due to dehydration of the agarose gel such that the useful lifetime of these phantoms is between one to ten hours. In brief, agarose phantoms are phantoms with short lifetime but disposable and easily reproducible [35].

There are a few problems regarding to the construction of solid phantoms:

- If the amount of agarose is insufficient, the mixture is not hardened even in a few hours.
- If the microspheres suspended in water are mixed with epoxy-resin, the mixture is not homogeneous as the water containing the spheres is float on top of the epoxy-resin. Drying the aqueous solution of microspheres, one can extract the particles. Drying the solution however may cause the particles to clump or may change their optical properties. Aqueous microspheres however can be used directly in agarose phantoms.
- The concentration of the scatterers in the agarose phantoms cannot be determined precisely as the amount of water changes during the heating up process.

If the agarose solution is heated too strongly, the solution may literally get burnt. This will be indicated by the cloudy colour of the solution.

4. CONCLUSIONS

In this paper, we have demonstrated the necessity for using different materials in phantom construction for different applications. We describe the procedures for making: (a) epoxy-resin dispersed homogeneous phantom composed of gold microspheres that can be used to find the point spread function of the system and longitudinal/transverse resolutions of an OCT system (b) epoxy-resin homogeneous phantoms composed of polystyrene microspheres that can be used to evaluate the optical properties extraction algorithm. Additionally, we discuss the relative merits of each of these types of phantom.

Acknowledgements

We thank Professor Ian Bruce. Adrian Bradu from the Applied Optics Group (AOG) of University of Kent for his valuable input.

REFERENCES

- [1] M. Firbank, "The design, calibration and usage of a solid scattering and absorbing phantom for near infra red spectroscopy", Ph.D thesis submitted to the University of London (1994).
- [2] M. Firbank, M. Oda, and D. T. Delpy, "An Improved Design for a Stable and Reproducible Phantom Material for Use in Near Infrared Spectroscopy and Imaging," *Phys. Med. Biol.* 40, 955-955 (1995).
- [3] Medical physics homepage, http://www.medphys.ucl.ac.uk/research/borl/research/NIR_topics/phantoms.htm, last accessed May 2011
- [4] S. Madsen, M. Patterson, and B. Wilson, "The use of India ink as an optical absorber in tissue-simulating phantoms," *Phys. Med. Biol.* 37, 985-993 (1992).
- [5] U. Sukowski, F. Schubert, D. Grosenick, and H. Rinneberg, "Preparation of solid phantoms with defined scattering and absorption properties for optical tomography," *Phys. Med. Biol.* 41, 1823-1844 (1996).
- [6] A. Agrawal, T. J. Pfefer, N. Gilani and R. Drezek, "Three-dimensional characterization of optical coherence tomography point spread functions with a nanoparticle-embedded phantom," *Opt. Lett.*, vol. 35, pp. 2269-2271, 2010.
- [7] C. E. Bisailon, G. Lamouche, R. Maciejko, M. Dufour and J. P. Monchalain, "Deformable and durable phantoms with controlled density of scatterers," *Phys. Med. Biol.*, vol. 53, pp. N237, 2008.
- [8] B. F. Kennedy, S. Loitsch, R. A. McLaughlin, L. Scolaro, P. Rigby and D. D. Sampson, "Fibrin phantom for use in optical coherence tomography," *J. Biomed. Opt.*, vol. 15, pp. 030507, 2010.
- [9] D. M. de Bruin, R. H. Bremmer, V. M. Kodach, R. de Kinkelder, J. van Marle, T. G. van Leeuwen and D. J. Faber, "Optical phantoms of varying geometry based on thin building blocks with controlled optical properties," *J. Biomed. Opt.*, vol. 15, pp. 025001, 2010.
- [10] P. D. Woolliams, R. A. Ferguson, C. Hart, A. Grimwood and P. H. Tomlins, "Spatially deconvolved optical coherence tomography," *Appl. Opt.*, vol. 49, pp. 2014-2021, 2010.
- [11] B. W. Pogue and M. S. Patterson, "Review of tissue simulating phantoms for optical spectroscopy, imaging and dosimetry," *J. Biomed. Opt.* 11, 041102 (2006).
- [12] X. Huang, P. K. Jain, I. H. El-Sayed, and M. A. El-Sayed, "Gold nanoparticles: interesting optical properties and recent applications in cancer diagnostics and therapy," *Nanomedicine* 2, 681-693 (2007).

- [13] A. M. Schmitt, "Principles and Application of Optical Coherent Tomography in Dermatology." *Dermatology*, vol. 217, pp. 12, 2008.
- [14] C. BOHREN and D. HUFFMAN, "Absorption and scattering of light by small particles," *Research Supported by the University of Arizona and Institute of Occupational and Environmental Health. New York, Wiley-Interscience, 1983, 541 p*, 1983.
- [15] M. Yadlowsky, J. Schmitt and R. Bonner, "Multiple scattering in optical coherence microscopy," *Appl. Opt.*, vol. 34, pp. 5699-5707, 1995.
- [16] L. Thrane, "Optical coherence tomography: modeling and applications," PhD thesis, 2001.
- [17] E. Hecht and A. Zajac, "Optics", Addison-Wesley Pub. Co: ISBN: 0201028352, 4th edition (2003)
- [18] J. Gordon, "Simple method for approximating Mie scattering," *Journal of the Optical Society of America A*, vol. 2, pp. 156-159, 1985.
- [19] Steven L. Jacques, Scott A. Prahl, Optical properties. At : <http://omlc.ogi.edu/classroom/ece532/class3/index.html>, last accessed May 2011
- [20] D. Levitz, "Determining tissue optical properties with optical coherence tomography," MSC thesis, 2004.
- [21] Schott, TIE-29: Refractive Index and Dispersion, Technical Information. Schott AG, 2007.
- [22] X. Ma, J. Q. Lu, R. S. Brock, K. M. Jacobs, P. Yang, and X. H. Hu, "Determination of complex refractive index of polystyrene microspheres from 370 to 1610 nm," *Phys. Med. Biol.* 48, 4165-4172 (2003).
- [23] C. Bohren and D. Huffman, "Absorption and scattering of light by small particles," *Research Supported by the University of Arizona and Institute of Occupational and Environmental Health. New York, Wiley-Interscience, 1983, 541 p*, 1983.
- [24] Epoxy-resin provider, <http://www.robnor.co.uk>, last accessed May 2011.
- [25] D. Levitz, C. B. Andersen, M. H. Frosz, L. Thrane, P. R. Hansen, T. M. Jorgensen and P. E. Andersen, "Assessing blood vessel abnormality via extracting scattering coefficients from OCT images," *Proceedings of SPIE*, vol. 5140, pp. 12, 2003.
- [26] W. Drexler, *Optical Coherence Tomography: Technology and Applications. Book*, Springer Verlag, 2008.
- [27] L. Thrane, M. H. Frosz, T. M. Jørgensen, A. Tycho, H. T. Yura, and P. E. Andersen, "Extraction of optical scattering parameters and attenuation compensation in optical coherence tomography images of multilayered tissue structures," *Opt. Lett.* 29, 1641-1643, 2004.
- [28] Bays, R.; Wagnieres, G.; Robert, D.; Theumann, J. F.; Vitkin, A.; Savary, J. F.; Monnier, P.; van den Bergh, H. Three-dimensional optical phantom and its application in photodynamic therapy. *Lasers Surg. Med.* **1997**, *21*, 227-234.

- [29] Chern, R. L.; Liu, X. X.; Chang, C. C. Particle plasmons of metal nanospheres: Application of multiple scattering approach. *Physical Review E*, no. 76, 16609, 2007.
- [30] Optical properties of Indian ink, <http://www.sennelier.fr/>, last accessed May 2011.
- [31] M. Canpolat and J. R. Mourant, "Optical measurement of photosensitizer concentration using a probe with a small source-detector fiber separation," in *Proceedings of SPIE*, 2000, pp. 10.
- [32] Pro-Jet 900NP data sheet, http://www.fujifilm.eu/fileadmin/products/Imaging_Colorants/Data_Sheets/Infra-Red_Absorbers/Pro-Jet_900NP.PDF, last accessed May 2011.
- [33] Agarose provider, <http://www.melford.co.uk>, last accessed May 2011.
- [34] Mohammad R.N. Avanaki, A. Hojjatoleslami, A. Braudo, and A. Gh. Podoleanu, "Optical parameter extraction towards skin cancer diagnosis", *Proceeding of International conference on microscopy, Microscience 2010*, pp.152, 2010.
- [35] Mohammad R.N. Avanaki, A. Hojjatoleslami, and A. Gh. Podoleanu, "Design and construction of multilayer tissue-like optical phantom", *Proceeding of International conference on microscopy, Microscience 2010*, pp.155, 2010.
- [36] M. Hughes, "High Lateral Resolution Imaging with Dynamic Focus", PhD thesis, university of Kent, 2010